Surface Functionalization

International Edition: DOI: 10.1002/anie.201504920
German Edition: DOI: 10.1002/ange.201504920

Efficient Photochemical Approaches for Spatially Resolved Surface Functionalization

Guillaume Delaittre, Anja S. Goldmann, Jan O. Mueller, and Christopher Barner-Kowollik**

Keywords:
macromolecular chemistry · modular ligation · photochemistry · surfacemodification · surface patterning

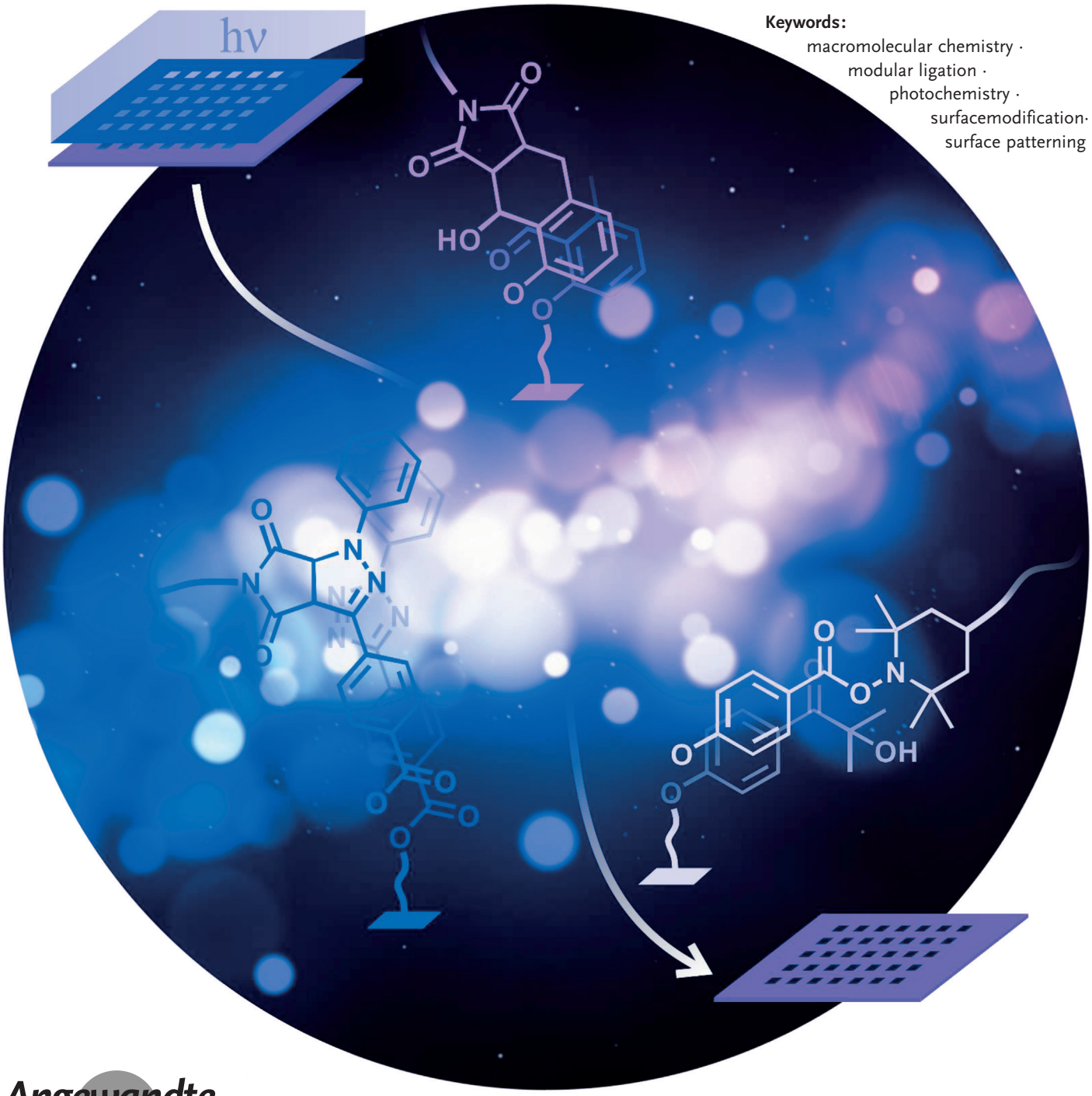

Materials interfaces—with a gas, a liquid, or another solid—are highly important for advanced applications. Besides their topological design, controlling interactions at these interfaces is typically realized by tuning the chemical composition of the materials surface. In areas such as nanoscience or biology, it is, however, highly desirable to impart heterogeneously distributed properties. Photopatterning, more than micro- and nanoprinting methods, is often the method of choice for precise functionalization, especially in terms of versatility. Recently, a range of new or rediscovered photochemistry approaches have been applied to precision surface functionalization, with the common aim of increasing efficiency and resolution while concomitantly lowering the amount of required energy. A survey of such methods is presented in this Review, with a focus on those we have explored.

From the Contents

1. Introduction

The use of light as a trigger for chemical reactions has fascinated scientists for decades. Through evolution, nature—a master of photochemistry—has optimized complex photochemical processes that contain valuable lessons for today's chemists. A possible definition of the key criteria an ideal photoinduced reaction should fulfill includes low-energy activation (visible light), high quantum yields, no catalyst, quantitative conversion under equimolar reaction conditions, facile synthesis, and (bio)orthogonality. Clearly, these are demanding requirements and not many reactions fulfill all the criteria.

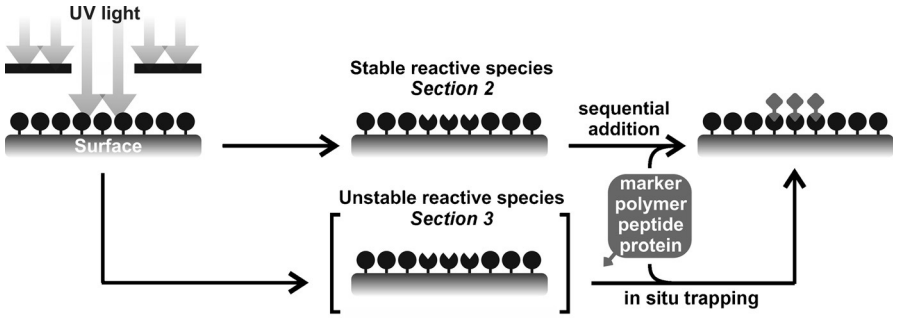

Scheme 1. Graphical representation of the two overarching categories of photochemical patterning methods described in this Review.

Although several reviews on photochemistry in the context of material science exist,[1] we present here the photochemical strategies explored in our laboratory as well as selected related examples from others. We have concentrated our efforts on the surface modification of inorganic substrates as well as biopolymers. In several cases, especially for inorganic substrates, a premodification step—either silanization or dopamine-based coating—was carried out. In the last five years, we have especially focused on methods that can be sorted into two categories: 1) efficient coupling after photodeprotection of one of the reaction partners and 2) phototriggered generation of highly reactive species which cannot be isolated under conventional conditions but can be trapped in situ (Scheme 1). Besides these methods, one should mention the revival of methods based on catalyst photoactivation (e.g. photoacids and photobases),[2] for example, the photoinduced copper-catalyzed azide-alkyne cycloaddition.[3] However, for the sake of brevity, we have structured the present Review in agreement with the two aforementioned categories. It is important to note that all the photochemical steps described below proceed at ambient temperature and that, unless otherwise stated, the photoactive moieties are bound to the surface to be patterned. This last aspect ensures a maximal lateral resolution by preventing diffusion of reactive species out of the irradiated areas.

For each strategy, we aim to provide insights with respect to the criteria characterizing an ideal photochemical reaction.

[*] Dr. G. Delaittre, Dr. A. S. Goldmann, J. O. Mueller, Prof. Dr. C. Barner-Kowollik
Preparative Macromolecular Chemistry
Institut für Technische Chemie und Polymerchemie
Karlsruhe Institute of Technology (KIT)
Engesserstrasse 18, 76131 Karlsruhe (Germany)
E-mail: guillaume.delaittre@kit.edu
christopher.barner-kowollik@kit.edu

Dr. G. Delaittre
Institute of Toxicology and Genetics (ITG)
Karlsruhe Institute of Technology (KIT)
Hermann-von-Helmholtz-Platz 1
76344 Eggenstein-Leopoldshafen (Germany)

Dr. A. S. Goldmann, J. O. Mueller, Prof. Dr. C. Barner-Kowollik
Institut für Biologische Grenzflächen
Karlsruhe Institute of Technology (KIT)
Hermann-von-Helmholtz-Platz 1
76344 Eggenstein-Leopoldshafen (Germany)

2. Photodeprotection of Caged Reactive Moieties for Highly Efficiently Coupling

Group protection is typically employed to protect part of a molecule which is sensitive to the conditions of a reaction that is carried out at a different site.[4] Although most protecting groups and their methods of cleavage rely on chemical activation, there is growing interest in photocaging, that is, protecting chemical functions with a moiety which can be removed by photoirradiation.[5] This method was pioneered in the area of surface patterning by Fodor et al. in the 1990s[6] and has also proved valuable in biological contexts.[7] Various photoremovable groups have been designed and it is now possible to remove two photocaging groups independently from the same molecule by employing distinct wavelengths.[8] In Section 2 we give an overview of patterning methods which make use of such protecting groups. An example where a photodecarbonylation/dehydrogenation is involved—but not precisely based on a protecting group—is also presented in Section 2.3.

2.1. o-Nitrobenzyl-Photoactivated Carbonyl-Nucleophile Additions

o-Nitrobenzyl—along with *o*-nitroveratryl, a derivative for longer wavelengths—is arguably the most popular photocaging moiety. Alcohols,[9] amines,[10] thiols,[11] and carboxylic acids[12] can be generated upon photocleavage of their corresponding *o*-nitrobenzyl ethers, carbamates, thioethers, and esters. However, these common moieties are not very reactive and need an additional catalyst to act in fast and efficient reactions. In 2008, Park and Yousaf reported photoactive self-assembled monolayers (SAMs) in which photocaged aminooxy groups were involved.[13] Aminooxy compounds typically react with carbonyl moieties in an oxime ligation,[14] a versatile method in bioconjugation and materials science. Thus, a disulfide compound bearing an aminooxy terminal group was capped with 4,5-dimethoxy-2-nitrobenzyl chloroformate to yield the photoreleasable nucleophile group (6 steps, 28% yield). Spatially resolved deprotection using masked irradiation at $\lambda = 365$ nm for 60 min was carried out in a saturated solution of semicarbazide. This additive is required to trap the nitrosobenzaldehyde by-product, which is formed during photocleavage and could react directly with the unveiled aminooxy groups. Sequential patterned deprotection and incubation steps with various keto-fluorophores enabled the generation of multicolor patterns. Gradient-like deprotection and subsequent oxime-based immobilization were achieved by using a lithographic mask. Eventually, keto-modified cell-adhesive peptides were patterned on a mixed SAM containing the photocaged aminooxy alkanethiol and tetraethylene glycol alkanethiol, which provided a globally cell-repellent background. Unfortunately, no experimental details were given with regard to the duration of the oxime ligation after deprotection. Shortly after, Maynard and coworkers reported a similar approach, which did not require any additive during the photoactivation step.[15] Indeed, they

Guillaume Delaittre heads an independent research group at the Karlsruhe Institute of Technology (KIT). He obtained his PhD for studies on polymerization-induced self-assembly with Prof. B. Charleux. After postdoctoral research with Profs. R. J. M. Nolte and J. J. L. M. Cornelissen at the Radboud University Nijmegen, the Netherlands, he obtained an Alexander-von-Humboldt Fellowship to work with Profs. C. Barner-Kowollik and M. Bastmeyer on advanced 3D cell substrates. Besides his interest in photopatterning, his research focuses on reactive nanostructured materials and enzyme–polymer hybrid systems.

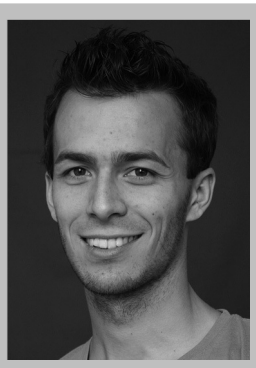

Jan Mueller obtained his Diploma in chemistry at the KIT in 2011 under the supervision of Prof. C. Barner-Kowollik. He is currently pursuing a PhD in the field of light-induced ligation techniques for application in polymer chemistry and materials science in the same group. His research interests focus on advancing the features of light-triggered and cycloaddition-based conjugation techniques.

Anja Goldmann completed her PhD in 2010 under the supervision of Prof. A. H. E. Müller at the University of Bayreuth. Her research projects during her PhD focused on click chemistry and its application in complex macromolecular architecture and surface modification. Since 2010, she has been the research manager in the group of Prof. C. Barner-Kowollik at the KIT. Her research interests include novel efficient ligation techniques, functional polymers, and their application to (bio)surface modification and materials science.

Christopher Barner-Kowollik received a PhD in Physical Chemistry in 1999 with Prof. M. Buback (Göttingen University). After postdoctoral research and academic positions at the Centre for Advanced Macromolecular Design at the University of New South Wales in Sydney, he was appointed Full Professor of Polymer Chemistry in 2006 at the same institution. Since 2008 he has held the chair for Macromolecular Chemistry at the KIT and is Professor of Materials Science at the Queensland University of Technology (QUT). His research interests include macromolecular precision design in solution and on surfaces by light-triggered methods.

synthesized in seven steps (yield of 17%) an alkanethiol in which the aminooxy fragment was linked to the *o*-nitrobenzyl group at the β-position.[5a] As a result, no aldehyde is formed. Instead, an *o*-nitro-α-methylstyrene derivative is released, which may have some implications in other setups.

For this reason, we took a reverse approach compared to traditional photo-uncaging. Indeed, instead of considering the nitrosobenzaldehyde formed during photocleavage as a by-product, we employed it as the coupling moiety of interest.[16] As an additional benefit, aldehydes can also be involved in another efficient and highly regarded ligation, namely hydrazone formation.[17] We thus investigated the possibility of attaching an *o*-nitroveratryl derivative to surfaces through its aromatic fragment to yield aldehyde patterns for subsequent oxime ligation. For this purpose, we designed a highly labile *o*-nitroveratryl ether derivative in which one of the methoxy substituents attached to the phenyl ring was replaced to incorporate a carboxylic acid anchoring group (5 steps, 15% overall yield, Figure 1a). The carboxylic acid group was exploited for linking the new photoreactive group to a polymer strand to investigate the kinetics and product structure in solution as well as for anchoring it onto silicon wafers through silanization. Complete cleavage of the ether was realized in 3 min under very mild conditions (370 nm, 18 W, ambient temperature), as proven by electrospray ionization mass spectrometry (ESI-MS). Along with the expected main product, we also identified a few species arising from nitroso-based side reactions. Although this method does not seem to be sufficiently clean for solution-based coupling, it is perfectly suitable for attachment to surfaces, as all the products possess the necessary aldehyde group. Simply shaking the deprotection products in the presence of hydroxylamine hydrochloride overnight at ambient temperature resulted in quantitative formation of the oxime. As expected, the surface reaction performed at least as well as the liquid-phase experiments. After coating the silicon wafers with the *o*-nitrobenzylethersilane, they were irradiated through a metallic mask (Figure 1b). After 3 min of irradiation, X-ray photoelectron spectroscopy (XPS) revealed complete disappearance of the nitro group in the irradiated zone. The NO_2^- ion map obtained by time-of-flight secondary ion mass spectrometry (ToF-SIMS) reproduced the mask structure with high fidelity (Figure 1c,d). Reaction of the partially deprotected wafers with *O*-((perfluorophenyl)methyl)hydroxylamine hydrochloride (PFPMHA)—a model compound highly suitable for ToF-SIMS imaging thanks to its halogen atoms—as well as with a Gly-Arg-Gly-Ser-Gly-Arg peptide (GRGSGR) bearing an aminooxy group at its N-terminus was then carried out. XPS showed the unambiguous increase in fluorine content on the wafer surface after the reaction with PFPMHA. ToF-SIMS showed the presence of fluorine atoms only in the previously irradiated areas in the case of the PFPMHA reaction (Figure 1c) as well as for peptide fragments in the case of GRGSGR (Figure 1d).

Overall, the oxime-based strategy—although it may suffer from the multistep synthesis of the photoactive species and a few side products—proved highly interesting as the energy input is rather low and the photoreaction is decoupled from the coupling step, which may be an advantage when highly sensitive compounds are involved.

A variant of this method was recently reported by Cha and co-workers in the frame of hydrazone chemistry.[18] Instead of an aldehyde, a ketone was produced upon irradiation of an *o*-nitrobenzyl ether molecule that was bound at its aromatic site to silicon micropillars. The ketone groups were then treated with hydrazide-functionalized DNA and a hydrazine-labeled antibody. In contrast to the oxime formation, which does not require a catalyst, it was necessary to employ an aromatic amine (*m*-phenylenediamine) to ensure efficient coupling. The formed hydrazone bond is sensitive to acidic conditions and requires an

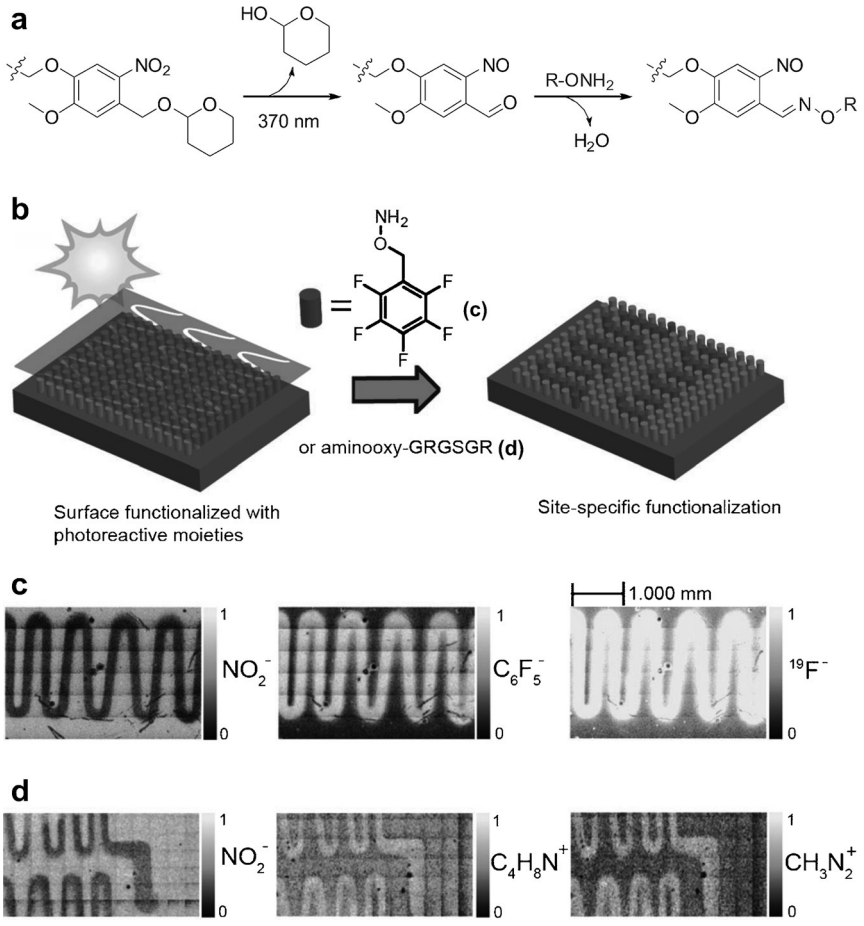

Figure 1. a) Synthetic route to phototriggered oxime ligation. b) Schematic representation of the oxime ligation-based photopatterning technique. c), d) Ion maps obtained by ToF-SIMS after patterning of PFPMHA and aminooxy-GRGSGR, respectively. Adapted from Ref. [16].

additional reducing treatment to become entirely stable. Nevertheless, the reversibility of this linkage could be considered as an advantage in some applications.

2.2. 1,3-Dipolar Azide-Cycloalkyne Cycloaddition Mediated by Cyclopropenyl Photodecarbonylation

One of the most popular coupling techniques in contemporary materials chemistry is the 1,3-dipolar azide-alkyne cycloaddition (AAC).[19] The copper-catalyzed version has been widely used to generate a broad range of polymeric materials.[20] For this variant, a method in which the active Cu^{I} species is generated through UV irradiation has been reported.[3] However, as previously mentioned, it may ultimately suffer from diffusion effects that would affect the resolution. Nevertheless, AAC can be performed without the need for a catalyst if strained[21] or electron-deficient[22] alkynes are used. A method based on the photogeneration of these types of alkynes or azides would thus be desirable. Unfortunately, azides are usually not photostable.[23] However, Poloukhtine and Popik showed that alkynes could be formed by photolysis of cyclopropenones.[24] In addition, Garcia-Garibay and co-workers reported quantum yields for the photodecarbonylation of diarylcyclooctynes which could reach unity in solution and even larger than three in the crystalline state thanks to a chemical amplification phenomenon.[25] Interestingly, the most widely employed strained cyclooctyne motif—although it has now been surpassed in terms of reactivity[26] and ease of synthesis[27]—is dibenzocyclooctyne (DBCO), a diarylcyclooctyne.[28] Locklin, Popik, and co-workers thus developed a patterning method based on the photogeneration of a DBCO derivative for subsequent strain-promoted azide-alkyne cycloaddition (SPAAC; Figure 2a).[29] Here, polymer brushes were grown from silicon wafers by copper-catalyzed reversible-deactivation radical polymerization (CuRDRP)[30] and subsequently modified to incorporate a diarylcyclopropenone derivative. The kinetics of deprotection of the DBCO group in the polymer brushes were monitored by UV/Vis spectroscopy, and it was found that full conversion was achieved in no more than 150 s ($\lambda =$ 350 nm, 3.5 mW cm^{-2}), with 95% of the cyclopropenone deprotected after 90 s. Finally, a binary pattern of fluorophores could be obtained by two consecutive irradiation/AAC sequences, with each cycloaddition step requiring an hour of immersion in the corresponding azido dye (Figure 2b–d). All in all, the phototriggered strain-promoted azide-alkyne cycloaddition seems robust and highly efficient. It does, however, suffer from a tedious synthetic route for the preparation of the cyclopropene-protected DBCO component. SPAAC is sometimes described as a slow reaction. Although it was never explored in the context of surface chemistry, cycloadditions of nitrones[28] and electron-deficient aryl azides[31] onto strained alkynes were found to be significantly faster than those of aliphatic azides classically employed in SPAAC.

2.3. Nucleophilic Amine-Phthalimide Addition Mediated by Photodecarbonylation/Dehydrogenation of Maleimide-Phencyclone Diels–Alder Adducts

While the approaches reported above rely on moieties which are not present in naturally occurring biomolecules and can, therefore, be recognized as biorthogonal to some extent, this is not the case for oxime ligation involving carbohydrates. In some cases, the carbohydrates may not be suitable as reactive counterparts and need to be specifically designed and synthesized. Thus, it may be desirable to develop a method to pattern peptides purely consisting of canonical amino acids. We employed a route based on the photo-decarbonylation/dehydrogenation of a phencyclone-maleimide Diels–Alder cycloadduct (Figure 3a).[32] This simple strategy implies that any type of substrate possessing a maleimide handle can be rendered photoreactive towards amino compounds by simply treating the former with a slight excess of a phencyclone derivative. Through a short screening of phencyclone structures, we found that 1,3-bis(4-methoxyphenyl)-2*H*-cyclopenta-[l]phenanthren-2-one (MCPO) performed the best. This method was first evaluated in solution, with a maleimido-peptide (Mal-Pep) that was treated with MCPO. The cycloadduct was quantitatively formed from a nearly stoichiometric mixture (1:1.05 mol/mol). This step can be readily monitored by UV/Vis spectroscopy and even visually, as MCPO is strongly absorbing at $\lambda = 644$ nm and forms a dark green solution. After 40 h of incubation at ambient temperature with Mal-Pep, no residual absorbance can be measured at $\lambda = 644$ nm and the solution becomes colorless. The subsequent photoinduced decomposition of the MCPO-Mal-Pep cycloadduct is carried out at

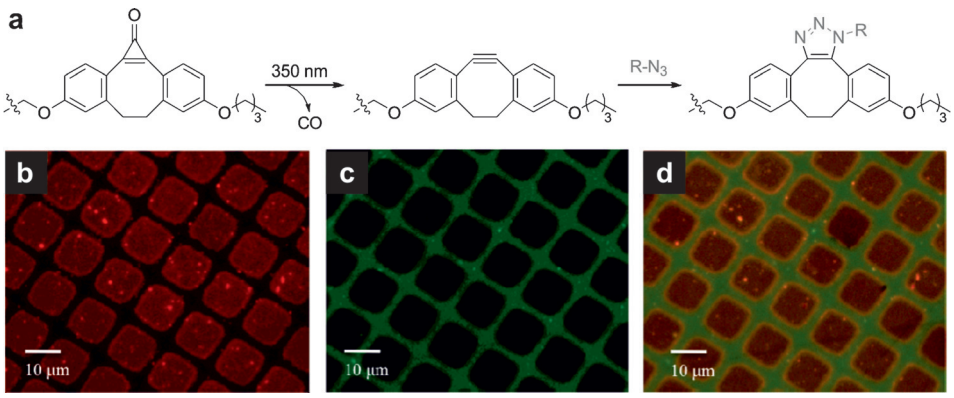

Figure 2. a) Synthetic route to phototriggered SPAAC. Fluorescence microscopy images of glass slides patterned by SPAAC with an azido-Lissamine rhodamine B conjugate and azidofluorescein: $\lambda_{ex} = 550$ nm (b), 447 nm (c), and 350 nm (d). Adapted from Ref. [29] with permission from the American Chemical Society.

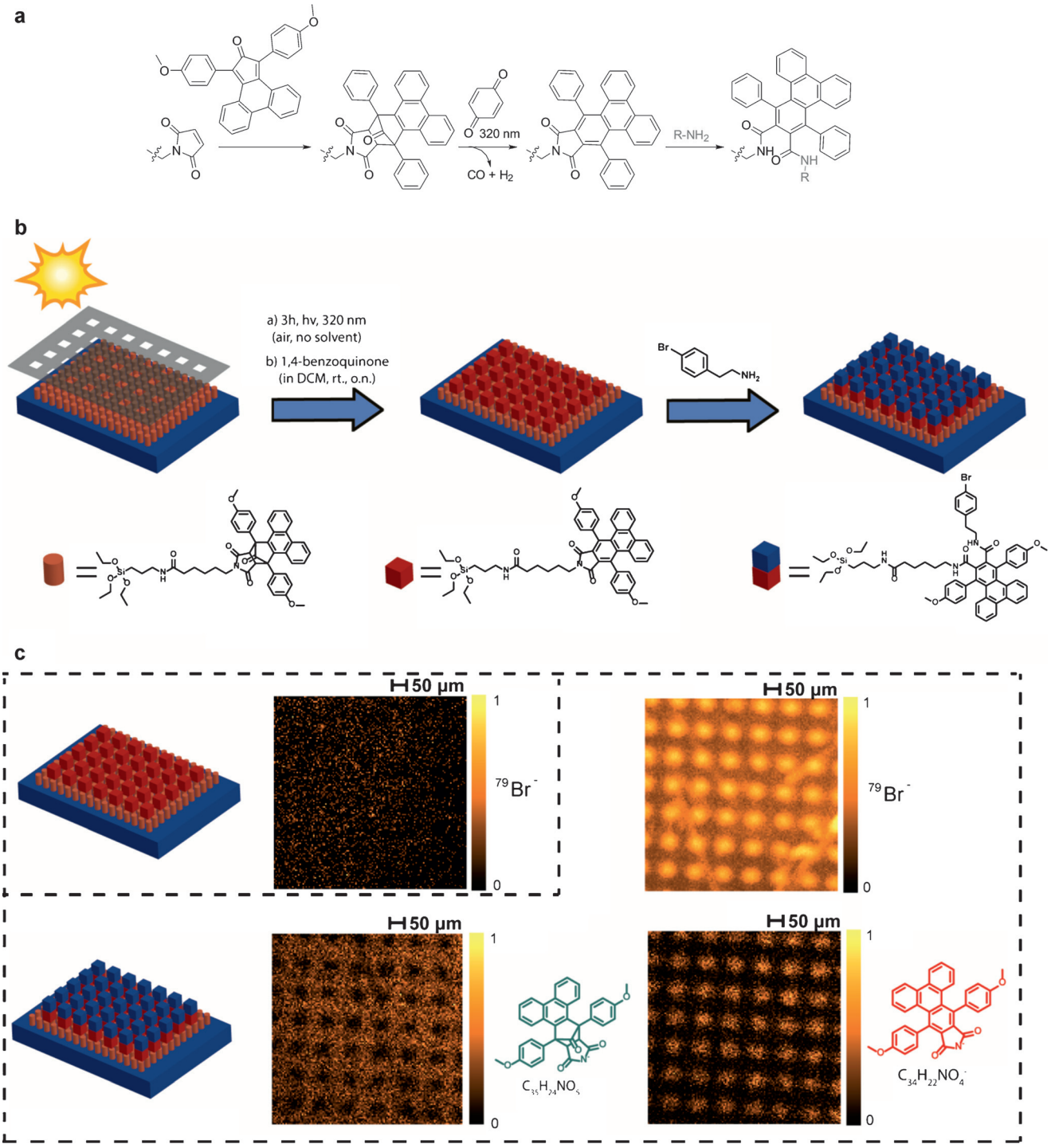

Figure 3. a) Synthesis of a maleimide-phencyclone cycloadduct, photoactivaton, and subsequent amine grafting. b) Corresponding patterning strategy. c) Ion maps obtained by ToF-SIMS showing the photodecarbonylation/dehydrogenation step as well as amine grafting. Adapted from Ref. [32].

$\lambda = 320$ nm (36 W) and is complete within 2 h. After this period of time, elimination of carbon monoxide and hydrogen yields a rearomatized phthalimide-like compound (triphenylene imide) which is susceptible to nucleophilic attack with amines. For complete dehydrogenation, it is necessary to employ an excess of 1,4-benzoquinone. A clear disadvantage of this strategy is that a very large excess of amines (typically *x*00-fold) is required for complete consumption of the triphenylene imide. Although this is a problematic feature for solution-based applications, it does not constitute a major hurdle for surface patterning, especially as non-irradiated phencyclone-maleimide adducts are stable in the presence of a vast excess of amines. Thus, a photoactive silane was readily synthesized from a maleimide-silane and MCPO and coated onto silicon wafers, thereby allowing patterning of 2-(4-fluorophenyl)ethanamine, which is easily detected by ToF-

SIMS (Figure 3b). The photoactivation step was characterized individually, as it was possible to distinguish secondary ions arising from the cycloadduct and its decarbonylated/dehydrogenated counterpart, respectively (Figure 3c). We then showed that a cell-adhesive cyclic peptide possessing a pendent lysine group (c(RGDfK)), as well as a highly charged statherin peptide sequence, could be patterned. A control reaction with a thiol compound not bearing any amine moiety was negative, thus showing an interesting selectivity with regard to the cysteine motif.

3. Phototriggered Generation of Unstable Species and their In Situ Trapping

There is a fine, yet clear, line between the photodeprotection methods reported in Section 2 and the photoactivation techniques detailed below. Indeed, the photoinduced event at the molecular level is still generally a cleavage (except in Section 3.4). However, the following methods are distinguished by the intrinsic instability of the released moieties.

3.1. Addition and Trapping Reactions of Photogenerated Radicals

Carbon radicals are reactive species and are usually associated with high reaction rates. However, radical reactions rarely rely on equimolar ratios. Nevertheless, these methods are popular, as the starting materials are readily accessible. Typically, radicals can be generated from the photolysis of photoinitiators.[33] The use of photoinitiators provides a key advantage, as tuning the wavelength can be carried out by selecting the appropriate photoinitiator. Photoredox catalysts have also been employed to generate carbon radicals.[34]

Important examples of phototriggered radical coupling reactions, including for surface functionalization, are thiol-ene and thiol-yne radical additions.[35] Both rely on the same mechanism: A carbon radical is created from an initiator (typically in catalytic amounts); this radical abstracts a hydrogen atom from a thiol, thereby creating a thiyl radical that is capable of adding onto an alkene. The addition yields another radical that is able to abstract a thiol proton and restart the cycle.[36] Depending on the olefin, side reactions such as polymerization can compete. An interesting variant of this approach for hydrogel patterning was recently reported in which allyl sulfides replaced simple alkenes, thereby allowing reversible patterning by an addition-fragmentation-transfer mechanism.[37] The reaction with alkynes proceeds identically to that with alkenes, except that a double addition is possible, which consequently leads to attachment of two thiols onto one alkynylated scaffold. Since the radical of interest (thiyl) is produced by a bimolecular process, these methods can suffer from a lack of spatial resolution, as radicals can migrate out of the irradiation zone. Depending on the desired feature size of the pattern, this may however not be an issue, especially if one exploits oxygen inhibition.[38]

To circumvent this potential complication, we worked with a system that relies on the direct coupling of the primary carbon radicals arising from the photoinitiator. Indeed, when the radical-producing molecule is bound to a surface, the coupling can only occur at the site of irradiation and maximal lateral resolution can be achieved. As a radical source, we employed a simple photoinitiator, Irgacure 2959, which was anchored to diverse substrates.[39] To efficiently functionalize these substrates, we made use of radical spin traps based on 2,2,6,6-tetramethyl-piperidin-1-yl)oxyl (TEMPO). We investigated the kinetics of the reaction in solution through polymer–polymer coupling and found it proceeded to near quantitative conversion within 30 min at ambient temperature ($\lambda_{max} = 311$ nm, 36 W). This nitroxide spin trapping method was then transferred to cellulosic filter paper, the primary alcohols of which were esterified with a carboxylated Irgacure 2959 derivative. We were then able to graft TEMPO-end-functionalized polystyrene (PS) onto the cellulose substrate and increase its contact angle to 86° within 20 min of irradiation (10 min on each side). XPS clearly showed the presence of polystyrene at the surface (Figure 4).

Studer and co-workers adapted this strategy to the functionalization of polymer brushes obtained by surface-initiated nitroxide-mediated polymerization[40] of 2-hydroxy-2-methyl-1-(4-vinylphenyl)propan-1-one, a styrene derivative able to play the dual role of monomer and photoinitiator.[41] Irradiation (LED, $\lambda = 365$ nm) was performed over 4–5 h in the presence of biotinylated, perfluorinated, or triethylene glycol bearing TEMPO derivatives to yield the modified brushes, as evident by water contact angle measurements, XPS, and a streptavidin assay. A similar strategy was applied to the functionalization of zeolites.[42]

Owing to the large range of commercially available or reported TEMPO derivatives, as well as the tolerance of many reactive groups towards radicals, the photoinduced radical-trapping method is extremely versatile with regard to patterned molecules. For example, proteins are routinely labeled with TEMPO.[43] In addition, the grafting is potentially reversible, as the formed alkoxyamine C–ON bond is thermally labile. Nevertheless, the small range of functional photoinitiators may limit applications, depending on the required irradiation wavelength. Another disadvantage is the sensitivity of the system towards oxygen species.

3.2. Cycloadditions and Nucleophilic Additions with Thioaldehydes Arising from the Photolysis of Phenacyl Sulfides

Thioaldehydes are highly reactive species, which in most cases are unstable and cannot be isolated.[44] These intermediates have been extensively studied and reviewed.[45] Their existence is classically evidenced through the formation of Diels–Alder adducts by in situ trapping with dienes (Figure 5a).[46] One way of producing thioaldehydes is by photolysis of phenacylsulfide (PhS) derivatives. Vedejs et al. were the first to thoroughly report the formation of thioaldehyde Diels–Alder adducts following the photolysis of phenacylsulfides.[47] A few years ago, we investigated the possibility

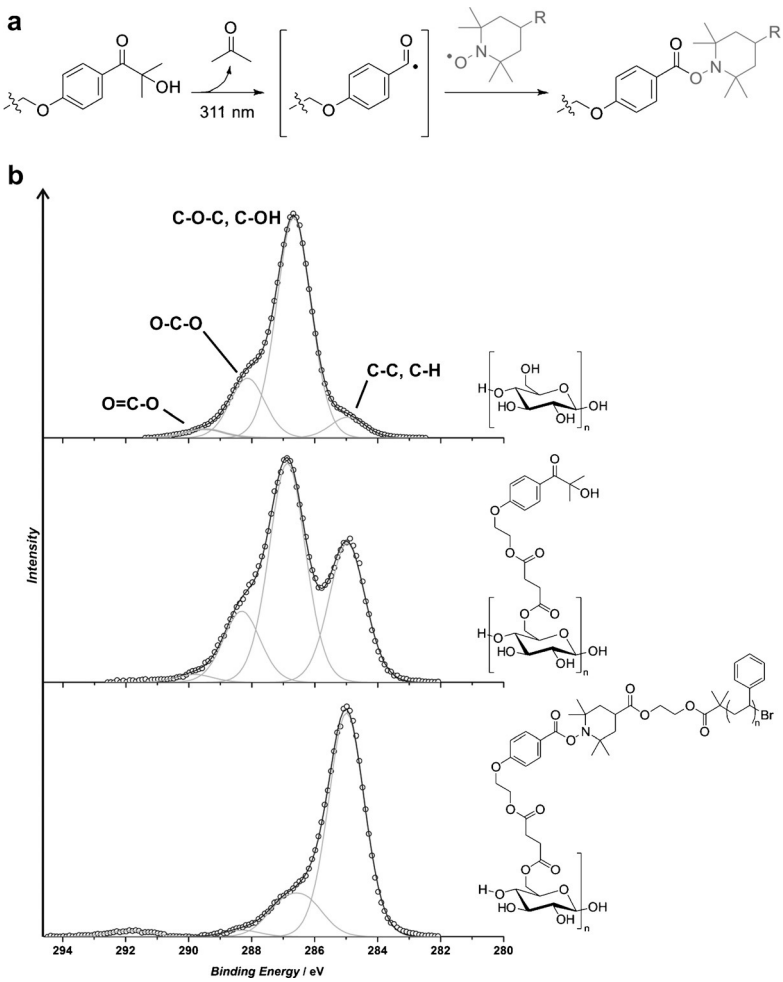

Figure 4. a) Schematic depiction of the phototriggered nitroxide spin trapping method. b) C1s XPS data showing the successful functionalization of cellulose with Irgacure 2959 (from top to middle) and spin trapping based polystyrene grafting (from middle to bottom). Adapted from Ref. [39] with permission from the American Chemical Society.

of functionalizing surfaces by using this method. An ESI-MS study in solution with a phenacylsulfide-capped poly(ethylene glycol) (PEG-PhS) model first showed that the reaction proceeded to completion in 20–30 min when using a 36 W compact low-pressure fluorescent lamp ($\lambda_{max} = 355$ nm) and an open-chain diene with an electron-withdrawing group (*trans*,*trans*-2,4-hexadienoic acid). This result suggests even faster kinetics for more reactive dienes, such as cyclopentadienyl derivatives.[48] A silane derivative of the phenacylsulfide was synthesized to equip silicon wafers with latent thioaldehydes. XPS analysis demonstrated that irradiation of the PhS-functionalized surfaces in the presence of cyclopentadienyl-capped PEG (PEG-Cp) induced grafting of a polymer layer. The same experiment was repeated with a photomask and led to well-defined structured immobilization, as proven by ToF-SIMS. We also demonstrated that this approach was applicable to biopolymer-based materials.[49] Cellulose was esterified with the PhS derivative employed to prepare PEG-PhS and tandem XPS/ToF-SIMS characterization ascertained the spatially constrained grafting of maleimide derivatives of a cell-adhesive peptide and of a fluorinated polymer.

Very recently, we also used our PhS photoplatform in a 1,3-dipolar cycloaddition-based strategy. Indeed, Vedejs, Houk, and co-workers also reported that photogenerated thioaldehydes can be trapped by nitronate esters with yields up to 90%.[50] Analogous to nitronate esters, nitrile oxides are rarely stable. Most of the time they are generated in situ from oximes, as in the case of a 1,3-dipolar cycloaddition with alkynes.[51] However, Schaumann and Rühter reported a stable nitrile oxide (mesitonitrile oxide, MNO) that was reactive towards thermally generated thioaldehydes.[52] We thus tested MNO, as well as a brominated counterpart, for the trapping of the thioaldehyde photogenerated from PEG-PhS (Figure 5a).[53] Irradiation (36 W, $\lambda_{max} = 355$ nm) for 30 min was sufficient for complete conversion with a PhS/MNO ratio of 1:5. Further ESI-MS investigations revealed that the reaction also reaches full conversion with equimolar amounts and a longer irradiation of 120 min. Following this success, several functional ether derivatives of 2-hydroxy-6-methylbenzonitrile oxide were synthesized as new, stable nitrile oxides and were patterned using a similar procedure as the aforementioned Diels–Alder route. Functionalities included a hydroxy-terminated alkane, benzoic acid, a butoxycarbonyl (Boc) protected amine, as well as a tertiary halogenoalkane. The last was further employed to yield a pattern of polymer brushes by CuRDRP. All the experiments were validated by XPS and ToF-SIMS analyses.

A further reaction of thioaldehydes which has been seldom reported is that with nucleophiles.[54] Thioaldehydes can react with amines and thiols to form imines,[55] disulfides,[56] and oximes (Figure 5a). It is interesting to note that an appropriate choice of the nucleophile would enable control over the reversibility of the immobilization, as imines,[57] oximes,[58] and disulfides[59] can be cleaved under specific conditions. In solution, PEG-PhS reacted quantitatively with two molar equivalents of a nucleophile within an hour.[60] Amines gave rise to two products: the expected imine and a thioamide arising from the oxidation of the imine by sulfur species. Reactions with thiols afforded the disulfide with good yields in an oxidizing environment after reaction in the presence of *N*,*N*-diisopropylethylamine (DIPEA). Aminooxy compounds gave the clearest outcome, with only one product formed in the absence of any additive. Finally, similarly to the aforementioned approaches based on thioaldehydes, photopatterning was demonstrated with nucleophiles such as amino-PEG, 4-bromobenzylmercaptan, and *O*-(2,3,4,5,6-pentafluorobenzyl)hydroxylamine hydrochloride.

The nucleophilic variant of the thioaldehyde-mediated patterning was further exploited in the area of cross-linked nanolayers, analogues of 2D polymers.[61] Indeed, one method

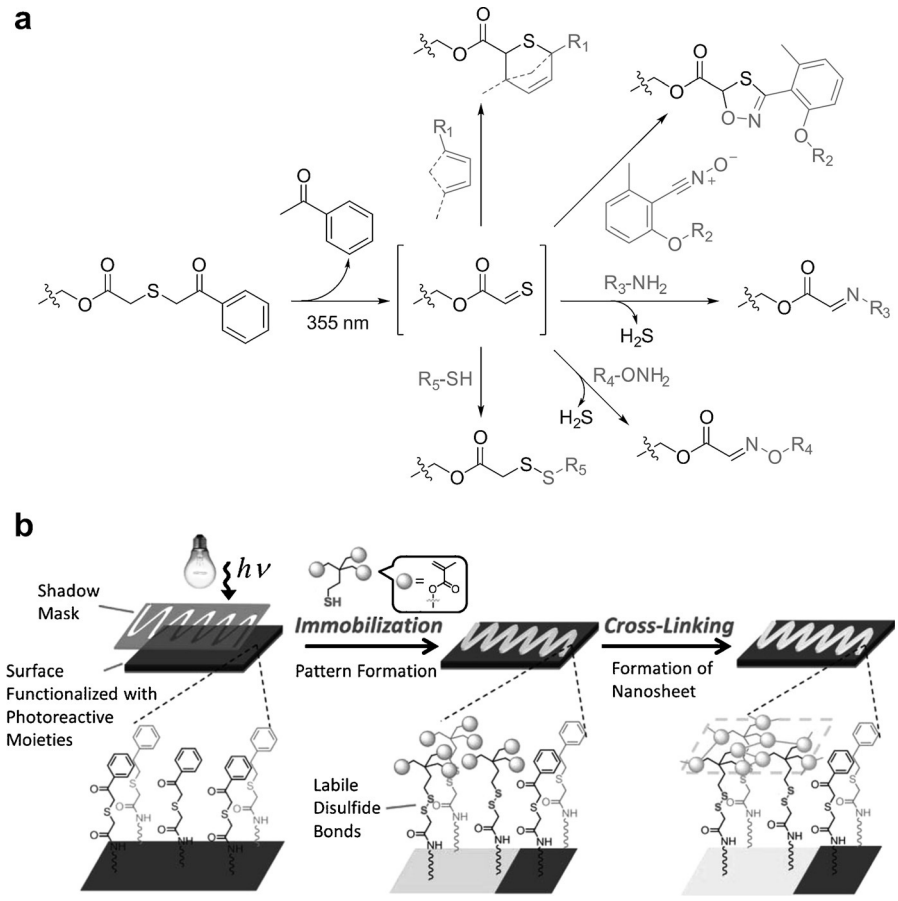

Figure 5. a) Generation of a thioaldehyde by photolysis of a phenacyl sulfide derivative and subsequent trapping reactions described in Section 3.2. b) Schematic depiction of the method employed for the synthesis of a 2D polymer based on patterning of a thiol-containing trimethacrylate (TMA-SH). Reproduced from Ref. [62] with permission from the American Chemical Society.

to produce such polymers is to conduct a polymerization of multifunctional monomers at an interface, where they are preassembled. Thus, a trimethacrylate possessing a thiol group (TMA-SH) was immobilized on a PhS-coated silicon wafer. This provided a cross-linking precursor layer that was bound to the surface through a labile disulfide bridge, which would potentially enable release of the nanolayers at a later stage (Figure 5b).[62] We carried out two preliminary experiments: 1) one in solution through irradiation of a model PhS derivative and TMA-SH and 2) another one consisting of an unpatterned grafting of TMA-SH on a PhS-modified silicon wafer. ESI-MS and XPS supported our synthetic design. Interestingly, it was shown that DIPEA was not mandatory for the reaction to proceed. Silicon wafers were then decorated with TMA-SH by masked irradiation. At this stage, two distinct routes were employed to cross-link surface-bound TMA-SH modules: 1) direct radical polymerization of the methacrylate units initiated by azobis(isobutyronitrile) (AIBN) or copolymerization with 2,2,2-trifuoroethyl methacrylate (TFMA); or 2) Diels–Alder cycloaddition with a tetrafunctional linker based on photoenol precursors (see Section 3.4). For the homo-cross-linking homopolymerization of TMA units, ToF-SIMS revealed the presence of anions characteristic of AIBN only in the irradiated areas, which further corroborates the efficient thioaldehyde-based photopatterning. The fluorine-containing ion maps also rigorously reproduced the pattern in the case of the cross-linking copolymerization with TFMA. Photoenol-based cross-linking required an additional pre-cross-linking step: Indeed, since this method is based on the photogeneration of dienes, irradiation may also induce cross-linking in the previously masked areas. Therefore, irradiation in the presence of 2,3-dimethylbutadiene was performed to first neutralize these domains and this was followed by cross-linking with the photoenol multifunctional linker. ToF-SIMS confirmed the disappearance of phenacylsulfide over the entire surface, and also showed 2-formyl-3-methylphenoxide anions characteristic of the photoenol cross-linker exclusively in the areas where TMA-SH was initially patterned. Together with a conclusive S_2^- ion map, these results show that the disulfide bonds generated from the thioaldehyde-based photocycloaddition are stable under these conditions.[62]

The strategies based on the photogeneration of thioaldehyde present the disadvantage of a reduced selectivity, but are easy to implement as phenacylsulfide derivatives are very simple to produce. The side product of the photocleavage step, acetophenone, is so far considered to be benign.

3.3. Nitrile Imine Mediated Tetrazole-Ene Cycloaddition (NITEC)

Nitrile imines are another type of highly reactive species which, depending on their exact structure, can rarely be isolated. Notably, Huisgen, Sustmann, and co-workers reported as early as 1967 that 2,5-diaryltetrazoles can thermally or photolytically generate nitrile imines together with nitrogen (Figure 6a).[63] These species have since then only been observed by spectroscopic methods at low temperatures[64] or in the solid state.[65] Nevertheless, it was found that they can efficiently be trapped by numerous dipolarophiles to form five-membered cycloadducts (pyrazolines). This chemistry has in recent years been revisited by Lin and co-workers in the area of biochemistry and chemical biology.[66] The range of dipolarophiles of interest extends from non-activated alkenes and alkynes—such as allyl ethers[67] and even polybutadiene[68]—to strained olefins (norbornene,[69] cyclopropene[70]) and electron-deficient alkenes, such as (meth)acrylics[71] and fumarates.[72] We were the first to assess the potential of this

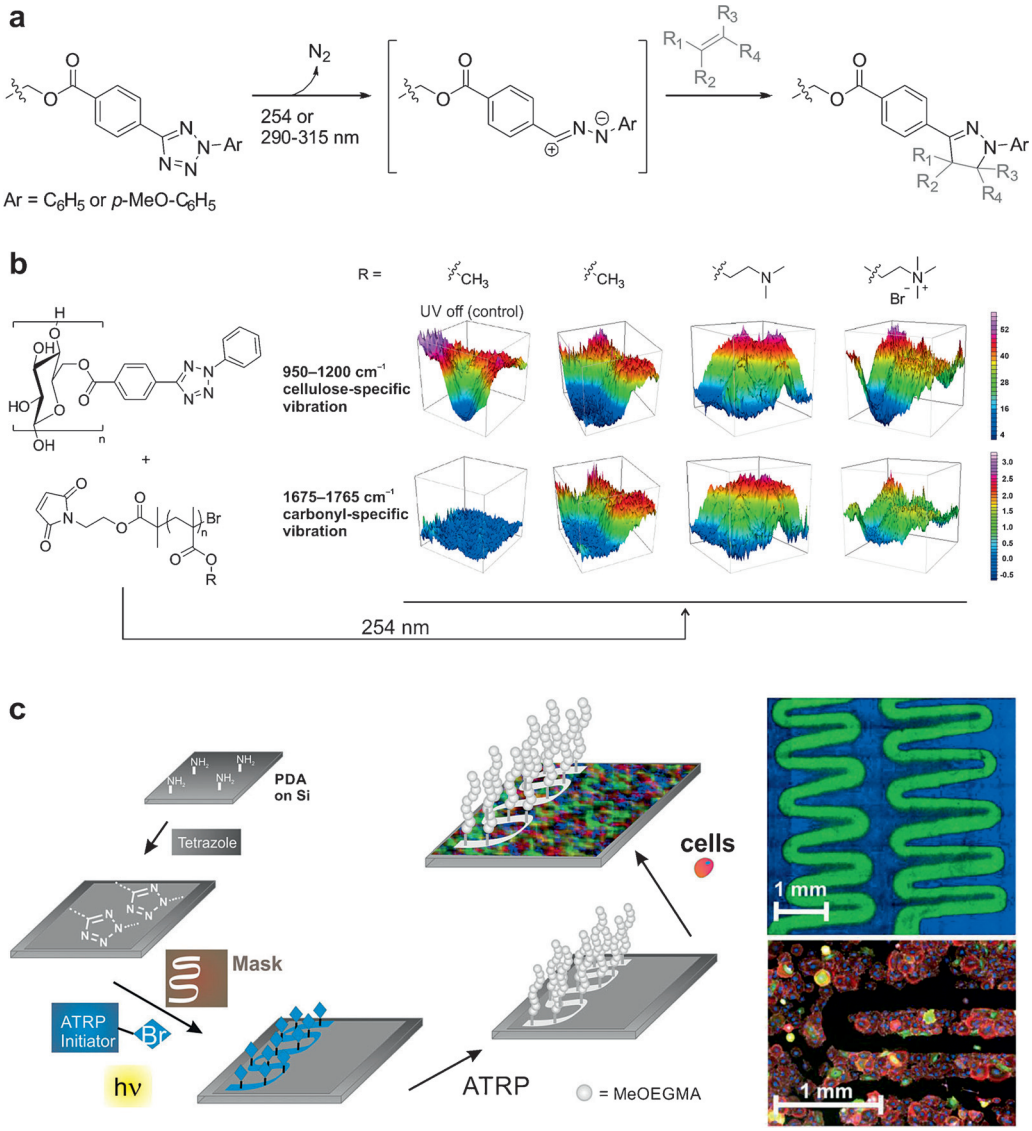

Figure 6. a) Mechanism of NITEC. b) FTIR microscopy data showing the patterning of diaryltetrazole-functionalized cellulose with various maleimide-capped polymethacrylates. Adapted from Ref. [73]. c) Patterning of non-fouling polymers onto polydopamine by NITEC and CuRDRP with subsequent ToF-SIMS characterization and cell culture assay. Adapted from Ref. [82].

method in the areas of polymer chemistry and surface modification and coined the term NITEC (nitrile imine mediated tetrazole-ene cycloaddition) to describe it.[73] We initially worked with the simplest type of diaryltetrazole, that is, with no substituent on the *N*-phenyl ring. In this case, the absorption maximum is located in the UVC[74] region, and experiments were carried out using a hand-held UV lamp irradiating at $\lambda = 254$ nm. We showed in a demanding polymer–polymer coupling experiment (equimolar ratios) that nearly quantitative formation of a block copolymer could be attained in just 20 min by using a tetrazole-functionalized PEG (PEG-Tet) and various maleimide-capped polymers. Upon realization that this method held great promise for the grafting of polymers onto surfaces—an application that requires short reaction times and high yields[75]—we studied its applicability to inorganic and bioorganic surfaces. The same carboxytetrazole employed to produce PEG-Tet was used to esterify cellulose filter paper as well as to synthesize a silane derivative. In the latter case, XPS analysis validated the grafting of maleimido-poly(methyl methacrylate) (Mal-PMMA). In the case of cellulose, we varied the nature of the grafted polymer with features ranging from hydrophobicity (PMMA) to thermo- and pH-responsivity or bactericidal activity.

Macropatterning experiments could easily be visualized, as the pyrazoline cycloadduct exhibits strong fluorescence. As a complement to the XPS characterization, the success of the grafting reaction with polymethacrylates was evaluated by FTIR microscopy (Figure 6b). Indeed, it was possible to discriminate between control samples (incubation of the filters with a polymer solution without irradiation) and the grafted samples, as the latter exhibited vibrations specific to both cellulose and the esters groups.

When we sought to adapt NITEC for the patterning of photoresponsive surfaces with azobenzene units, we found that a wavelength of $\lambda = 254$ nm was inadequate, but that the tetrazole could still be activated satisfactorily by using a low-power (9 W) lamp emitting in the UVB region (290–315 nm).[76] Maleimide derivatives bearing either one or two azobenzene motifs were attached and yielded domains that could reversibly undergo a change of wettability.

Later, NITEC was employed for the grafting of non-fouling polymers onto paper to develop attractive materials from sustainable resources. We used milder conditions and utilized a tetrazole derivative with a methoxy substituent at the *para* position of the *N*-phenyl ring.[77] This allowed us to work in the UVA region, which is a requirement for more sensitive biological systems, such as proteins. Again, cellulose was directly esterified to provide a photoreactive surface which was selectively modified with a bromoalkane able to

initiate CuRDRP. Subsequently, the surface-initiated polymerization of carboxybetaine acrylamide was carried out. ToF-SIMS and FTIR microscopy confirmed the spatial fidelity of the patterning step. In the same study, we also demonstrated the successful coating of paper with maleimide-tagged streptavidin (SAv). Since SAv is ubiquitously employed for the immobilization of various biomolecules, its patterning onto paper together with antifouling polymers paves the way for the development of microfluidic devices that operate through capillary forces.[78]

The NITEC procedure was also applied in conjunction with a biomimetic approach based on polydopamine (PDA), which is regarded as a synthetic analogue of melanin[79] and is obtained by the reaction of dopamine hydrochloride in Tris buffer (pH 8.1).[80] Amine moieties are available at the surface of PDA films and serve as handles for further modifications.[79,81] In analogy to our work with cellulose, we functionalized PDA with the methoxydiaryltetrazole compound and patterned a CuRDRP initiator (Figure 6c).[82] This time, brushes of oligoethylene glycol methyl ether methacrylate were grown. ToF-SIMS, XPS, and ellipsometry confirmed the success of the synthetic sequence. Finally, patterned surfaces were incubated with rat embryonic fibroblasts. Cells were found to strictly segregate within the non-irradiated zones and not to invade the PEGylated areas, thus demonstrating the high efficiency of the patterning approach.

NITEC-based photopatterning is powerful as it exhibits rather fast kinetics, but may suffer from a lack of strict orthogonality as nitrile imines are subject to nucleophilic attack. Nevertheless, it is highly efficient in aqueous media, particularly in biological environments,[66,70,83] when an adequate dipolarophile is present. Tetrazole precursors are relatively straightforward to obtain. In addition, NITEC is a profluorescent technique, which is particularly useful for imaging purposes.

3.4. Diels–Alder Cycloaddition of Photogenerated Transient Dienes

Although powerful in terms of efficiency, all the strategies described so far rely on reactive species that are formed irreversibly. This implies that, in the absence of a trapping partner, it can lead to an inactive moiety and, perhaps of a higher concern, undesired side products. Thus, a photoactivatable chemical group which can return to a dormant state when the light source is turned off and can again be switched on when desired is of high interest.

A few years ago, inspired by the seminal work of Meador et al.,[84] we introduced photogenerated *o*-quinodimethanes in the context of macromolecular engineering.[85] *o*-Quinodimethanes (or *o*-xylylenes) are species that can be generated under light from *o*-methylphenyl ketones and aldehydes, for example. They take part in an equilibrium with these structures and are thus considered as elusive or transient species (Figure 7a).[86] *o*-Quinodimethanes of this type are also termed photoenols—strictly speaking photodienols—and are very reactive dienes. They take part in fast Diels–Alder cycloadditions with molecules possessing an electron-deficient triple or double bond such as acetylenedicarboxlic esters,[84b] maleimides,[84a,85] fumarates,[87] acrylonitrile,[87] and acrylates,[84b,87] or even thiocarbonylthio compounds commonly used as transfer agents for RDRP as well as the polymers obtained thereby.[88] After we had envisaged applying photoenol chemistry for surface patterning, a screening of various *o*-methylphenyl ketones and aldehydes led to the identification of the 2-formyl-3-methylphenoxy (FMP) group as a more efficient latent photoenol than our previously reported 2-methylbenzophenone derivative.[85] Indeed, under optimized conditions, an FMP-capped PEG (PEG-FMP) reacted quantitatively with maleimide (10 equiv) within 15 min on irradiation at $\lambda = 320$ nm (36 W).[89] The same reaction in pure water under otherwise identical conditions took significantly longer, which is explained by the stabilization of the FMP-based photoenol in apolar solvents by hydrogen bonding in a six-membered cycle with the ether group at position 6 of the aromatic ring. An FMP silane derivative was subsequently synthesized and employed to coat silicon wafers. XPS revealed successful silanization and led us to investigate the ability of surface-bound FMP moieties to undergo Diels–Alder cycloadditions with maleimide derivatives. Monofunctionalization with the aforementioned CuRDRP initiator occurred within 2 h of irradiation, as shown by XPS and ToF-SIMS. Dual patterning of this initiator and maleimido-PEG (Mal-PEG) was also confirmed by ToF-SIMS through high-fidelity reproduction of the features of the metallic mask that was employed. Finally, we showed that a model peptide could be patterned by photoenol-mediated cycloaddition.

Encouraged by this initial success, we sought to merge the photoenol strategy with our interest in the modification of natural polymers, particularly cellulose and hyaluronan (HA).[90] The FMP moiety was covalently bound to cellulose filters as well as to tethered films of HA. Immobilization is a prerequisite for surface characterization of HA and to avoid surface desorption. This was achieved by amidification of aminated silicon wafers and confirmed by XPS as well as surface plasmon resonance spectroscopy and atomic force microscopy. Subsequent esterification of the primary hydroxy groups present in the repeating units of HA as well as of cellulose with a carboxy-FMP derivative was validated by XPS. Finally, ToF-SIMS and XPS measurements ascertained the local light-induced (320 nm, 36 W, 2 h) grafting of maleimido-PTFMA (Mal-PTFMA) and an antimicrobial peptide bearing a maleimide end group.

As noted in Section 3.3, a way of functionalizing not only silicon wafers or biopolymers but also any other type of surface is by coating with PDA. We thus designed a dopamine-like photoenol precursor, whereby a hydroxy-FMP derivative was esterified with a 3,4-dihydroxy-L-phenylalanine (L-DOPA) scaffold.[91] Poly(FMP-DOPA) films were then successfully obtained on gold, graphite, and polyethylene terephthalate (PET), as confirmed by water contact angle measurements: After coating, all the materials exhibited a similar advancing water contact angle of approximately 87°. XPS was employed to confirm the successful photoinduced global attachment of Mal-PEG and Mal-PTFMA onto gold and of a maleimido-Gly-Arg-Gly-Asp-Ser peptide

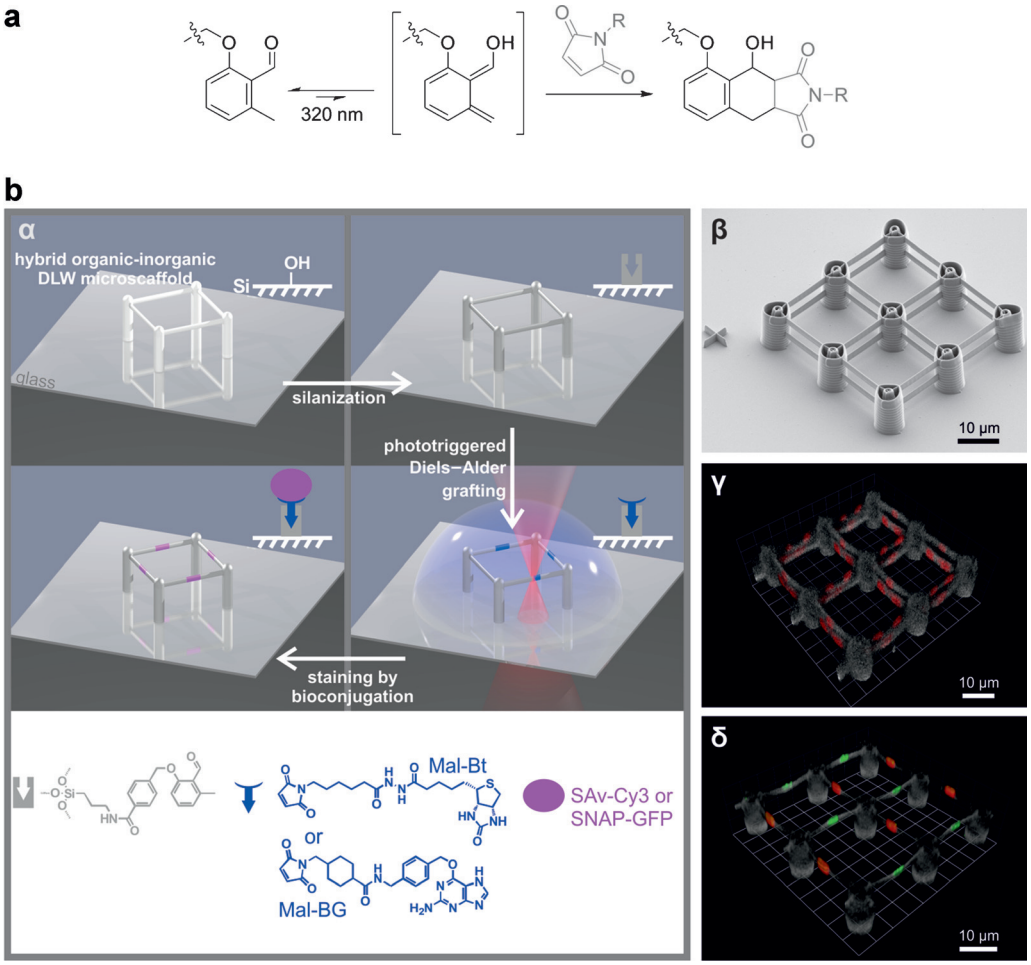

Figure 7. a) Photoenol-based Diels–Alder cycloaddition with maleimides. b) Two-photon-triggered functionalization of FMP-coated 3D microscaffolds with fluorescent proteins: α) Overall synthetic strategy; β) scanning electron micrograph of a 3D microstructure; γ) confocal fluorescence microscopy image of a 3D microscaffold after patterning of Mal-Bt and staining with a Cy3-labeled streptavidin; δ) confocal fluorescence microscopy image of a 3D microscaffold after patterning of Mal-Bt and Mal-BG and staining with Cy3-labeled streptavidin and SNAP-tagged green fluorescent protein. Adapted from Ref. [92].

onto gold and PET. It seems justified to claim that FMP-DOPA can be considered as a universal photoreactive coating agent.

Perhaps the most impressive display of the power of photoenol chemistry is its translation to multiphoton-based three-dimensional (3D) patterning (Figure 7b).[92] Two-photon pulsed laser irradiation enables the precise localization of a photochemical event in a drastically reduced volume (the focus of the laser), where the probability of a molecule to absorb two photons simultaneously is sufficiently high.[93] Consequently, a low-energy irradiation—typically a doubled wavelength, for example, in the infrared—can be employed and the surroundings of the laser focus are not affected. Nevertheless, not every photosensitive molecule is amenable to multiphoton excitation. The FMP moiety was, therefore, evaluated in this context using confocal fluorescence microscopy. Glass coverslips were first treated with the FMP-silane and were then subjected to two-photon irradiation in the presence of a biotinylated maleimide at various wavelengths (560–700 nm) in a custom-made direct laser writing (DLW) setup. A series of biotin line patterns with various spacings—to probe the resolution limit of our approach—were written with simultaneous variation of the laser power. The patterns were stained by incubating the slides in a solution of rhodamine-labeled avidin. Between the writing and staining steps, a flood irradiation in the presence of Mal-PEG was carried out to suppress unspecific protein adsorption around the biotinylated areas. The optimal wavelength for two-photon-induced Diels–Alder cycloaddition of FMP and maleimides is between $\lambda =$ 620 and 660 nm, which is about double the wavelength required for efficient one-photon excitation. Fluorescence reached a maximum for a laser power of 5 mW. As a consequence, we carried on employing this laser power at $\lambda =$ 640 nm. The experimental resolution lies somewhere between 1 and 2 μm. Thus, microscaffolds with overall sizes in the range of 10 to 20 μm and consisting of thick pillars holding two rows (referred to as lower and upper, respectively) of thin beams with a diameter of 2.5 μm were fabricated by two-photon polymerization using a commercial Nanoscribe DLW setup. The distance between the beams (surface to surface) is 2.5 μm. These microstructures are made of Ormocomp, an inorganic–organic hybrid photoresist which consists of organosilanes and silicon alkoxides. As a result, a silanization step similar to that carried out on silicon wafers could be employed to homogeneously coat the microstructures and make them entirely photoreactive (Figure 7bα). The next step was to reproduce the 2D glass-coverslip experiment in 3D. The same synthetic sequence was repeated with a pattern designed to show the high axial resolution. Indeed, lower and upper beams were irradiated at distinct coordinates in the *x*-*y* plane and axial (*z*) contamination was not observed (Figure 7bβ). We demonstrated the possibility of immobilizing three distinct components on the same scaffold: 1) a biotinylated maleimide (Mal-Bt) complexing a Cy3-labeled streptavidin

(SAv-Cy3), 2) a benzylguanine-functionalized maleimide (Mal-BG) inducing covalent attachment of a SNAP-tagged green fluorescent protein (SNAP-GFP), and 3) Mal-PEG-like species (Figure 7 bα). Several well-defined protein patterns with various configurations could be obtained (Figure 7 bγ). This work paves the way for highly elaborated 3D cell culture microdishes.

Although the photoreactive moieties were not initially immobilized on the surface to be patterned, it is worth noting the spatially resolved immobilization of gold nanoparticles (AuNPs, ca. 3 nm diameter), as it serves to illustrate a few appealing features of the photoenol approach.[94] Glass slides were silanized with a maleimide derivative while the FMP moiety was introduced onto the surface of AuNPs by esterification at the hydroxy group of the surface-bound mercaptoundecanol ligand. Approximately 10 FMP moieties were present on the surface of each AuNP. Micrometer-sized AuNP patterns were obtained using the aforementioned DLW setup operating at $\lambda = 700$ nm. Importantly, the amenability of photoenol chemistry for two-photon activation is an advantage in this context, as irradiation with a UVA laser may lead to the aggregation of AuNPs.[95] Following in-depth characterization of the FMP-AuNPs by high-resolution transmission electron microscopy, dynamic light scattering, as well as FTIR and NMR spectroscopies, a low laser power (0.2–0.4 mW) was employed, as aggregation was observed above 0.6 mW. This study highlights two important features of the photoenol mechanism: 1) the very short lifetime of the active species and 2) the reversible nature of the formation of these active species. Indeed, despite the fact that the photoactive molecules were able to diffuse, patterns with a resolution of approximately 1.5 μm could be achieved. In addition, although they were globally irra-

Table 1: Collation of the main characteristics of the photochemical methods described in this Review and tentative evaluation.

	Stable Reactive Intermediates					
Photogenerated species	Aminooxy	Aldehyde	Ketone	Cyclooctyne	Phthalimide-like	
Chemistry	Oxime Ligation	Oxime Ligation	Hydrazone Formation	SPAAC	Nucleophilic Ring-Opening	
Subsection in the text	2.1	2.1	2.1	2.2	2.3	
Employed wavelength*	365 nm	370 nm	?	350 nm	320 nm	
Additive	Semicarbazide*	-	*m*-phenylenediamine*	-	1,4-benzoquinone	
Side product of the photoirradiation	(*o*-nitrobenzaldehyde species or *o*-nitro-α-methylstyrene) + CO_2	tetrahydro-2*H*-pyran-2-ol	methanol	CO	CO, H_2	
Synthetic feasibility§						
Rate of photoreaction	?		?		?	
Product yield/equimolarity						
Selectivity						
Bioorthogonality						
Solvent compatibility						
Air compatibility						

	Unstable Reactive Intermediates						
Photogenerated species	Radical	Thioaldehyde	Thioaldehyde	Thioaldehyde	Nitrile Imine	*o*-Quinodimethane	*o*-Naphthoquinonemethide
Chemistry	Nitroxide Spin Trapping	Hetero-Diels–Alder Cycloaddition	1,3-Dipolar Cycloaddition	Nucleophilic Attack	1,3-Dipolar Cycloaddition	Diels–Alder Cycloaddition	Hetero-Diels–Alder Cycloaddition
Subsection in the text	3.1	3.2	3.2	3.2	3.3	3.4	3.4
Employed wavelength*	311 nm	355 nm	355 nm	355 nm	254-315 nm	320 nm	300 nm
Additive	-	-	-	-	-	-	-
Side product of the photoirradiation	Acetone	Acetophenone	Acetophenone	Acetophenone	N_2	-	H_2O
Synthetic feasibility§							
Rate of photoreaction							
Product yield/equimolarity							
Selectivity							
Bioorthogonality							
Solvent compatibility							
Air compatibility							

[*] These wavelengths are the ones which have been employed in the current examples. Nevertheless, for some of the reported strategies, a variation of the employed wavelengths was demonstrated in different contexts, often by tuning the chemical structure of the photoreactive species. [+] Only in Ref. [13]. [¥] Not during photoactivation, but for the subsequent coupling. [§] Taking into account both reaction partners. For the photoactive molecule, only the steps to convert a common functional group into the corresponding photoactive moiety are considered, not those to achieve a molecule that can be anchored to a surface.

diated during the patterning, immobilized FMP-AuNPs remained available for further photografting at their surface since photoenol moieties which did not take part in the surface attachment process simply returned to a latent state and could be employed for a subsequent photoreaction. To confirm this, a flood irradiation of the AuNP-grafted glass slide with a brominated maleimide was performed. The bromine ion map obtained by ToF-SIMS faithfully reproduced the gold ion map previously acquired.

This subsection would not be complete without mentioning a photoenol-related method developed by Popik, Locklin, and co-workers. Although the reversible generation of a diene resembles the photoenol strategy, this method is mechanistically different. Here, a 3-(hydroxymethyl)naphthalene-2-ol (NQMP) scaffold is dehydrated upon irradiation to form an *o*-naphthoquinonemethide (*o*NQM), which is a heterodiene that is highly reactive towards nucleophiles such as azide ions, thiols, or electron-rich dienes such as vinyl ethers and enamines in Diels–Alder cycloadditions.[96] This latter reactivity combined with the fact that any remaining *o*NQM moieties can be rehydrated under specific conditions in an aqueous medium makes it a close analogue and interesting complement to the photoenol technique. NQMP moieties were immobilized in a similar manner as the caged cyclooctynes described in Section 2.2.[97] Irradiation of these brushes in solutions of vinyl ether fluorophores at $\lambda =$ 300 nm through an electron microscopy grid for 1–2 min yielded clear fluorescent patterns. This chemistry proved orthogonal to both azides and alkynes, as demonstrated in a sequence including a first step of photopatterning of vinyl ether azide or alkyne derivatives followed by AAC with adequately functionalized fluorophores.

Although the reactive moieties NQMP and FMP are quite demanding in terms of synthetic effort, the reversible photogeneration of transient dienes is appealing as it is orthogonal to other methods: fully for the photoenols, while *o*-naphthoquinonemethides can also be involved in reversible reactions with thiols.[98] In addition, the reversible nature of the photoactivation is an advantage, particularly regarding the stability of the photoreactive surfaces.

4. Summary and Outlook

Today, we have at our disposal a range of powerful photochemically driven methods for the spatially resolved functionalization of diverse surfaces. These strategies are divided into those that allow photopatterning through stable yet reactive species and those which rely on intermediates that need to be trapped immediately. The employed method for surface functionalization must be carefully adjusted to the application. To provide a user guide to the strategies available, we have collated them in Table 1 according to their distinct advantages and disadvantages.

It is evident that none of the strategies described here offers all the features noted in the introduction. For example, although the method involving cyclopropenone-masked cyclooctynes is very efficient when one considers only reaction features, it suffers from a rather tedious synthetic route. In contrast, the phenacyl sulfide moiety is readily accessible, but the corresponding reactions can only be conducted under very specific conditions. In general, cycloaddition-based methods perform well in terms of kinetics and product yield.

The outstanding challenges that still need to be overcome include the efficient red-shifting of the excitation wavelengths. To date, very few photochemical ligation procedures exist that can be excited in the visible light regime, although this is highly desired in the realm of biological applications when operating with cellular systems or with complex biomolecules, for example. Equally important—although the first promising steps have been made in this direction[99]—is addressing different locations within one molecule or on one surface through photochemical reactions that respond to two different wavelengths while adhering as closely as possible to the criteria of an ideal photochemical ligation. Similarly, photochemical reactions have yet to be fully exploited for the generation of sequence-defined, monodisperse macromolecules,[100] be they in solution or tethered onto surfaces.

Acknowledgements

We are indebted to all the students, postdoctoral researchers, as well as scientific and technical staff members who contributed to the studies reported in this Review and developed many of the concepts currently employed in our laboratories. C.B.-K. acknowledges continued support from the Karlsruhe Institute of Technology (KIT) through both the state of Baden-Württemberg and the Helmholtz association, specifically the STN and BIFTM programs. G.D. thanks the German Federal Ministry of Education and Research (BMBF) for current funding.

How to cite: *Angew. Chem. Int. Ed.* **2015**, *54*, 11388–11403
Angew. Chem. **2015**, *127*, 11548–11564

[1] a) M.-M. Russew, S. Hecht, *Adv. Mater.* **2010**, *22*, 3348–3360; b) P. Yang, W. Yang, *Chem. Rev.* **2013**, *113*, 5547–5594; c) S. Chatani, C. J. Kloxin, C. N. Bowman, *Polym. Chem.* **2014**, *5*, 2187–2201; d) C. Bao, L. Zhu, Q. Lin, H. Tian, *Adv. Mater.* **2015**, *27*, 1647–1662.

[2] W. Xi, H. Peng, A. Aguirre-Soto, C. J. Kloxin, J. W. Stansbury, C. N. Bowman, *Macromolecules* **2014**, *47*, 6159–6165.

[3] B. J. Adzima, Y. Tao, C. J. Kloxin, C. A. DeForest, K. S. Anseth, C. N. Bowman, *Nat. Chem.* **2011**, *3*, 256–259.

[4] a) M. Schelhaas, H. Waldmann, *Angew. Chem. Int. Ed. Engl.* **1996**, *35*, 2056–2083; *Angew. Chem.* **1996**, *108*, 2192–2219; b) P. G. M. Wuts, T. W. Greene in *Greene's Protective Groups in Organic Synthesis*, *Fourth Edition,* John Wiley & Sons, Inc., New York, **2006**, pp. 1–15.

[5] a) C. G. Bochet, *J. Chem. Soc. Perkin Trans. 1* **2002**, 125–142; b) A. P. Pelliccioli, J. Wirz, *Photochem. Photobiol. Sci.* **2002**, *1*, 441–458.

[6] S. Fodor, J. Read, M. Pirrung, L. Stryer, A. Lu, D. Solas, *Science* **1991**, *251*, 767–773.

[7] P. Klán, T. Šolomek, C. G. Bochet, A. Blanc, R. Givens, M. Rubina, V. Popik, A. Kostikov, J. Wirz, *Chem. Rev.* **2012**, *113*, 119–191.

[8] C. G. Bochet, *Pure Appl. Chem.* **2006**, *78*, 241–247.

[9] A. G. Russell, M. J. Sadler, H. J. Laidlaw, A. Gutierrez-Loriente, C. W. Wharton, D. Carteau, D. M. Bassani, J. S. Snaith, *Photochem. Photobiol. Sci.* **2012**, *11*, 556 – 563.
[10] D. D. Young, A. Deiters, *Bioorg. Med. Chem. Lett.* **2006**, *16*, 2658 – 2661.
[11] a) G. Delaittre, T. Pauloehrl, M. Bastmeyer, C. Barner-Kowollik, *Macromolecules* **2012**, *45*, 1792 – 1802; b) T. Pauloehrl, G. Delaittre, M. Bastmeyer, C. Barner-Kowollik, *Polym. Chem.* **2012**, *3*, 1740 – 1749.
[12] a) N. Kotzur, B. Briand, M. Beyermann, V. Hagen, *Chem. Commun.* **2009**, 3255 – 3257; b) A. F. Hirschbiel, S. Geyer, B. Yameen, A. Welle, P. Nikolov, S. Giselbrecht, S. Scholpp, G. Delaittre, C. Barner-Kowollik, *Adv. Mater.* **2015**, *27*, 2621 – 2626.
[13] S. Park, M. N. Yousaf, *Langmuir* **2008**, *24*, 6201 – 6207.
[14] S. Ulrich, D. Boturyn, A. Marra, O. Renaudet, P. Dumy, *Chem. Eur. J.* **2014**, *20*, 34 – 41.
[15] R. J. Mancini, R. C. Li, Z. P. Tolstyka, H. D. Maynard, *Org. Biomol. Chem.* **2009**, *7*, 4954 – 4959.
[16] T. Pauloehrl, G. Delaittre, M. Bruns, M. Meißler, H. G. Börner, M. Bastmeyer, C. Barner-Kowollik, *Angew. Chem. Int. Ed.* **2012**, *51*, 9181 – 9184; *Angew. Chem.* **2012**, *124*, 9316 – 9319.
[17] R. Nguyen, I. Huc, *Chem. Commun.* **2003**, 942 – 943.
[18] J. H. Lee, D. W. Domaille, H. Noh, T. Oh, C. Choi, S. Jin, J. N. Cha, *Langmuir* **2014**, *30*, 8452 – 8460.
[19] H. C. Kolb, M. G. Finn, K. B. Sharpless, *Angew. Chem. Int. Ed.* **2001**, *40*, 2004 – 2021; *Angew. Chem.* **2001**, *113*, 2056 – 2075.
[20] a) G. Delaittre, N. K. Guimard, C. Barner-Kowollik, *Acc. Chem. Res.* **2015**, *48*, 1296—1307; b) L. Liang, D. Astruc, *Coord. Chem. Rev.* **2011**, *255*, 2933 – 2945.
[21] N. J. Agard, J. A. Prescher, C. R. Bertozzi, *J. Am. Chem. Soc.* **2004**, *126*, 15046 – 15047.
[22] M. Clark, P. Kiser, *Polym. Int.* **2009**, *58*, 1190 – 1195.
[23] N. Gritsan, M. Platz in *Organic Azides*, John Wiley & Sons, Ltd, Chichester, UK, **2010**, pp. 311 – 372.
[24] A. Poloukhtine, V. V. Popik, *J. Org. Chem.* **2003**, *68*, 7833 – 7840.
[25] G. Kuzmanich, M. N. Gard, M. A. Garcia-Garibay, *J. Am. Chem. Soc.* **2009**, *131*, 11606 – 11614.
[26] a) J. M. Baskin, J. A. Prescher, S. T. Laughlin, N. J. Agard, P. V. Chang, I. A. Miller, A. Lo, J. A. Codelli, C. R. Bertozzi, *Proc. Natl. Acad. Sci. USA* **2007**, *104*, 16793 – 16797; b) M. F. Debets, S. S. van Berkel, S. Schoffelen, F. P. J. T. Rutjes, J. C. M. van Hest, F. L. van Delft, *Chem. Commun.* **2010**, *46*, 97 – 99; c) J. C. Jewett, E. M. Sletten, C. R. Bertozzi, *J. Am. Chem. Soc.* **2010**, *132*, 3688 – 3690; d) M. F. Debets, J. S. Prins, D. Merkx, S. S. van Berkel, F. L. van Delft, J. C. M. van Hest, F. P. J. T. Rutjes, *Org. Biomol. Chem.* **2014**, *12*, 5031 – 5037.
[27] J. Dommerholt, S. Schmidt, R. Temming, L. J. A. Hendriks, F. P. J. T. Rutjes, J. C. M. van Hest, D. J. Lefeber, P. Friedl, F. L. van Delft, *Angew. Chem. Int. Ed.* **2010**, *49*, 9422 – 9425; *Angew. Chem.* **2010**, *122*, 9612 – 9615.
[28] X. Ning, J. Guo, M. A. Wolfert, G.-J. Boons, *Angew. Chem. Int. Ed.* **2008**, *47*, 2253 – 2255; *Angew. Chem.* **2008**, *120*, 2285 – 2287.
[29] S. V. Orski, A. A. Poloukhtine, S. Arumugam, L. Mao, V. V. Popik, J. Locklin, *J. Am. Chem. Soc.* **2010**, *132*, 11024 – 11026.
[30] a) B. M. Rosen, V. Percec, *Chem. Rev.* **2009**, *109*, 5069 – 5119; b) K. Matyjaszewski, *Macromolecules* **2012**, *45*, 4015 – 4039; c) M. Ouchi, T. Terashima, M. Sawamoto, *Chem. Rev.* **2009**, *109*, 4963 – 5050.
[31] J. Dommerholt, O. van Rooijen, A. Borrmann, C. F. Guerra, F. M. Bickelhaupt, F. L. van Delft, *Nat. Commun.* **2014**, *5*, 5378.
[32] T. Pauloehrl, A. Welle, M. Bruns, K. Linkert, H. G. Börner, M. Bastmeyer, G. Delaittre, C. Barner-Kowollik, *Angew. Chem. Int. Ed.* **2013**, *52*, 9714 – 9718; *Angew. Chem.* **2013**, *125*, 9896 – 9900.
[33] J. P. Fouassier, J. Lalevée in *Photoinitiators for Polymer Synthesis*, Wiley-VCH, Weinheim, **2012**, pp. 127 – 197.
[34] a) J. W. Tucker, C. R. J. Stephenson, *J. Org. Chem.* **2012**, *77*, 1617 – 1622; b) C. K. Prier, D. A. Rankic, D. W. C. MacMillan, *Chem. Rev.* **2013**, *113*, 5322 – 5363; c) J. Xuan, W.-J. Xiao, *Angew. Chem. Int. Ed.* **2012**, *51*, 6828 – 6838; *Angew. Chem.* **2012**, *124*, 6934 – 6944.
[35] a) P. Jonkheijm, D. Weinrich, M. Köhn, H. Engelkamp, P. C. M. Christianen, J. Kuhlmann, J. C. Maan, D. Nüsse, H. Schroeder, R. Wacker, R. Breinbauer, C. M. Niemeyer, H. Waldmann, *Angew. Chem. Int. Ed.* **2008**, *47*, 4421 – 4424; *Angew. Chem.* **2008**, *120*, 4493 – 4496; b) W. Feng, L. Li, E. Ueda, J. Li, S. Heißler, A. Welle, O. Trapp, P. A. Levkin, *Adv. Mater. Interfaces* **2014**, *1*, 1400269.
[36] a) C. E. Hoyle, C. N. Bowman, *Angew. Chem. Int. Ed.* **2010**, *49*, 1540 – 1573; *Angew. Chem.* **2010**, *122*, 1584 – 1617; b) A. B. Lowe, C. E. Hoyle, C. N. Bowman, *J. Mater. Chem.* **2010**, *20*, 4745 – 4750.
[37] N. R. Gandavarapu, M. A. Azagarsamy, K. S. Anseth, *Adv. Mater.* **2014**, *26*, 2521 – 2526.
[38] S. C. Ligon, B. Husár, H. Wutzel, R. Holman, R. Liska, *Chem. Rev.* **2014**, *114*, 557 – 589.
[39] G. Delaittre, M. Dietrich, J. P. Blinco, A. Hirschbiel, M. Bruns, L. Barner, C. Barner-Kowollik, *Biomacromolecules* **2012**, *13*, 1700 – 1705.
[40] J. Nicolas, Y. Guillaneuf, C. Lefay, D. Bertin, D. Gigmes, B. Charleux, *Prog. Polym. Sci.* **2013**, *38*, 63 – 235.
[41] A. Mardyukov, Y. Li, A. Dickschat, A. H. Schäfer, A. Studer, *Langmuir* **2013**, *29*, 6369 – 6376.
[42] T. Buscher, A. Barroso, C. Denz, A. Studer, *Polym. Chem.* **2015**, *6*, 4221 – 4229.
[43] W. L. Hubbell, H. S. McHaourab, C. Altenbach, M. A. Lietzow, *Structure* **1996**, *4*, 779 – 783.
[44] R. Okazaki in *Organosulfur Chemistry*, *Vol. 1* (Ed.: P. Philip), Academic Press, London, **1995**, pp. 225 – 258.
[45] a) E. Vedejs, *Acc. Chem. Res.* **1984**, *17*, 358 – 364; b) E. Vedejs, *J. Org. Chem.* **2004**, *69*, 5159 – 5167.
[46] a) A. Capperucci, A. Degl'Innocenti, A. Ricci, A. Mordini, G. Reginato, *J. Org. Chem.* **1991**, *56*, 7323 – 7328; b) A. Capperucci, A. Degl'Innocenti, T. Nocentini, G. Castagnoli, I. Malesci, A. Cerreti, *Phosphorus Sulfur Silicon Relat. Elem.* **2005**, *180*, 1247 – 1251.
[47] a) E. Vedejs, T. H. Eberlein, D. L. Varie, *J. Am. Chem. Soc.* **1982**, *104*, 1445 – 1447; b) E. Vedejs, T. H. Eberlein, D. J. Mazur, C. K. McClure, D. A. Perry, R. Ruggeri, E. Schwartz, J. S. Stults, D. L. Varie, *J. Org. Chem.* **1986**, *51*, 1556 – 1562; c) E. Vedejs, T. H. Eberlein, R. G. Wilde, *J. Org. Chem.* **1988**, *53*, 2220 – 2226.
[48] M. Glassner, K. K. Oehlenschlaeger, A. Welle, M. Bruns, C. Barner-Kowollik, *Chem. Commun.* **2013**, *49*, 633 – 635.
[49] T. Tischer, T. K. Claus, K. K. Oehlenschlaeger, V. Trouillet, M. Bruns, A. Welle, K. Linkert, A. S. Goldmann, H. G. Börner, C. Barner-Kowollik, *Macromol. Rapid Commun.* **2014**, *35*, 1121 – 1127.
[50] a) E. Vedejs, D. A. Perry, K. N. Houk, N. G. Rondan, *J. Am. Chem. Soc.* **1983**, *105*, 6999 – 7001; b) E. Vedejs, D. A. Perry, *J. Org. Chem.* **1984**, *49*, 573 – 575.
[51] I. Singh, Z. Zarafshani, J.-F. Lutz, F. Heaney, *Macromolecules* **2009**, *42*, 5411 – 5413.
[52] E. Schaumann, G. Rühter, *Tetrahedron Lett.* **1985**, *26*, 5265 – 5268.
[53] O. Altintas, M. Glassner, C. Rodriguez-Emmenegger, A. Welle, V. Trouillet, C. Barner-Kowollik, *Angew. Chem. Int. Ed.* **2015**, *54*, 5777 – 5783; *Angew. Chem.* **2015**, *127*, 5869 – 5875.
[54] V. A. Usov, L. V. Timokhina, M. G. Voronkov, *Sulfur Rep.* **1992**, *12*, 95 – 152.

[55] I. V. Zavarzin, V. N. Yarovenko, A. V. Shirokov, N. G. Smirnova, A. A. Es'kov, M. M. Krayushkin, *ARKIVOC* **2003**, *13*, 205 – 223.
[56] V. Duchenet, Y. Vallee, *J. Chem. Soc. Chem. Commun.* **1993**, 806 – 807.
[57] V. Saggiomo, U. Lüning, *Tetrahedron Lett.* **2009**, *50*, 4663 – 4665.
[58] J. Kalia, R. T. Raines, *Angew. Chem. Int. Ed.* **2008**, *47*, 7523 – 7526; *Angew. Chem.* **2008**, *120*, 7633 – 7636.
[59] R. Singh, G. M. Whitesides in *Sulphur-Containing Functional Groups (1993)*, John Wiley & Sons, Inc., Chichester, UK, **1993**, pp. 633 – 658.
[60] T. Pauloehrl, A. Welle, K. K. Oehlenschlaeger, C. Barner-Kowollik, *Chem. Sci.* **2013**, *4*, 3503 – 3507.
[61] J. Sakamoto, J. van Heijst, O. Lukin, A. D. Schlüter, *Angew. Chem. Int. Ed.* **2009**, *48*, 1030 – 1069; *Angew. Chem.* **2009**, *121*, 1048 – 1089.
[62] K. Fuchise, P. Lindemann, S. Heißler, H. Gliemann, V. Trouillet, A. Welle, J. Berson, S. Walheim, T. Schimmel, M. A. R. Meier, C. Barner-Kowollik, *Langmuir* **2015**, *31*, 3242 – 3253.
[63] J. S. Clovis, A. Eckell, R. Huisgen, R. Sustmann, *Chem. Ber.* **1967**, *100*, 60 – 70.
[64] N. H. Toubro, A. Holm, *J. Am. Chem. Soc.* **1980**, *102*, 2093 – 2094.
[65] S.-L. Zheng, Y. Wang, Z. Yu, Q. Lin, P. Coppens, *J. Am. Chem. Soc.* **2009**, *131*, 18036 – 18037.
[66] R. K. V. Lim, Q. Lin, *Acc. Chem. Res.* **2011**, *44*, 828 – 839.
[67] Y. Wang, W. Song, W. J. Hu, Q. Lin, *Angew. Chem. Int. Ed.* **2009**, *48*, 5330 – 5333; *Angew. Chem.* **2009**, *121*, 5434 – 5437.
[68] J. O. Mueller, N. K. Guimard, K. K. Oehlenschlaeger, F. G. Schmidt, C. Barner-Kowollik, *Polym. Chem.* **2014**, *5*, 1447 – 1456.
[69] Z. Yu, R. K. V. Lim, Q. Lin, *Chem. Eur. J.* **2010**, *16*, 13325 – 13329.
[70] Z. Yu, Y. Pan, Z. Wang, J. Wang, Q. Lin, *Angew. Chem. Int. Ed.* **2012**, *51*, 10600 – 10604; *Angew. Chem.* **2012**, *124*, 10752 – 10756.
[71] W. Song, Y. Wang, J. Qu, M. M. Madden, Q. Lin, *Angew. Chem. Int. Ed.* **2008**, *47*, 2832 – 2835; *Angew. Chem.* **2008**, *120*, 2874 – 2877.
[72] J. O. Mueller, D. Voll, F. G. Schmidt, G. Delaittre, C. Barner-Kowollik, *Chem. Commun.* **2014**, *50*, 15681 – 15684.
[73] M. Dietrich, G. Delaittre, J. P. Blinco, A. J. Inglis, M. Bruns, C. Barner-Kowollik, *Adv. Funct. Mater.* **2012**, *22*, 304 – 312.
[74] Y. Wang, W. J. Hu, W. Song, R. K. V. Lim, Q. Lin, *Org. Lett.* **2008**, *10*, 3725 – 3728.
[75] L. Nebhani, D. Schmiedl, L. Barner, C. Barner-Kowollik, *Adv. Funct. Mater.* **2010**, *20*, 2010 – 2020.
[76] E. Blasco, M. Piñol, L. Oriol, B. V. K. J. Schmidt, A. Welle, V. Trouillet, M. Bruns, C. Barner-Kowollik, *Adv. Funct. Mater.* **2013**, *23*, 4011 – 4019.
[77] T. Tischer, C. Rodriguez-Emmenegger, V. Trouillet, A. Welle, V. Schueler, J. O. Mueller, A. S. Goldmann, E. Brynda, C. Barner-Kowollik, *Adv. Mater.* **2014**, *26*, 4087 – 4092.
[78] X. Li, D. R. Ballerini, W. Shen, *Biomicrofluidics* **2012**, *6*, 011301.
[79] J. Liebscher, R. Mrówczyński, H. A. Scheidt, C. Filip, N. D. Hădade, R. Turcu, A. Bende, S. Beck, *Langmuir* **2013**, *29*, 10539 – 10548.
[80] H. Lee, S. M. Dellatore, W. M. Miller, P. B. Messersmith, *Science* **2007**, *318*, 426 – 430.
[81] R. Mrowczynski, L. Magerusan, R. Turcu, J. Liebscher, *Polym. Chem.* **2014**, *5*, 6593 – 6599.
[82] C. Rodriguez-Emmenegger, C. M. Preuss, B. Yameen, O. Pop-Georgievski, M. Bachmann, J. O. Mueller, M. Bruns, A. S. Goldmann, M. Bastmeyer, C. Barner-Kowollik, *Adv. Mater.* **2013**, *25*, 6123 – 6127.
[83] P. An, Z. Yu, Q. Lin, *Chem. Commun.* **2013**, *49*, 9920 – 9922.
[84] a) M. A. B. Meador, M. A. Meador, L. L. Williams, D. A. Scheiman, *Macromolecules* **1996**, *29*, 8983 – 8986; b) D. S. Tyson, F. Ilhan, M. A. B. Meador, D. D. Smith, D. A. Scheiman, M. A. Meador, *Macromolecules* **2005**, *38*, 3638 – 3646.
[85] T. Gruendling, K. K. Oehlenschlaeger, E. Frick, M. Glassner, C. Schmid, C. Barner-Kowollik, *Macromol. Rapid Commun.* **2011**, *32*, 807 – 812.
[86] J. L. Segura, N. Martín, *Chem. Rev.* **1999**, *99*, 3199 – 3246.
[87] B. Grosch, C. N. Orlebar, E. Herdtweck, W. Massa, T. Bach, *Angew. Chem. Int. Ed.* **2003**, *42*, 3693 – 3696; *Angew. Chem.* **2003**, *115*, 3822 – 3824.
[88] K. K. Oehlenschlaeger, J. O. Mueller, N. B. Heine, M. Glassner, N. K. Guimard, G. Delaittre, F. G. Schmidt, C. Barner-Kowollik, *Angew. Chem. Int. Ed.* **2013**, *52*, 762 – 766; *Angew. Chem.* **2013**, *125*, 791 – 796.
[89] T. Pauloehrl, G. Delaittre, V. Winkler, A. Welle, M. Bruns, H. G. Börner, A. M. Greiner, M. Bastmeyer, C. Barner-Kowollik, *Angew. Chem. Int. Ed.* **2012**, *51*, 1071 – 1074; *Angew. Chem.* **2012**, *124*, 1096 – 1099.
[90] T. Tischer, T. K. Claus, M. Bruns, V. Trouillet, K. Linkert, C. Rodriguez-Emmenegger, A. S. Goldmann, S. Perrier, H. G. Börner, C. Barner-Kowollik, *Biomacromolecules* **2013**, *14*, 4340 – 4350.
[91] C. M. Preuss, T. Tischer, C. Rodriguez-Emmenegger, M. M. Zieger, M. Bruns, A. S. Goldmann, C. Barner-Kowollik, *J. Mater. Chem. B* **2014**, *2*, 36 – 40.
[92] B. Richter, T. Pauloehrl, J. Kaschke, D. Fichtner, J. Fischer, A. M. Greiner, D. Wedlich, M. Wegener, G. Delaittre, C. Barner-Kowollik, M. Bastmeyer, *Adv. Mater.* **2013**, *25*, 6117 – 6122.
[93] a) M. Deubel, G. von Freymann, M. Wegener, S. Pereira, K. Busch, C. M. Soukoulis, *Nat. Mater.* **2004**, *3*, 444 – 447; b) C. N. LaFratta, J. T. Fourkas, T. Baldacchini, R. A. Farrer, *Angew. Chem. Int. Ed.* **2007**, *46*, 6238 – 6258; *Angew. Chem.* **2007**, *119*, 6352 – 6374.
[94] L. Stolzer, A. S. Quick, D. Abt, A. Welle, D. Naumenko, M. Lazzarino, M. Wegener, C. Barner-Kowollik, L. Fruk, *Chem. Commun.* **2015**, *51*, 3363 – 3366.
[95] S. Pocoví-Martínez, M. Parreño-Romero, S. Agouram, J. Pérez-Prieto, *Langmuir* **2011**, *27*, 5234 – 5241.
[96] S. Arumugam, V. V. Popik, *J. Am. Chem. Soc.* **2009**, *131*, 11892 – 11899.
[97] S. Arumugam, S. V. Orski, J. Locklin, V. V. Popik, *J. Am. Chem. Soc.* **2012**, *134*, 179 – 182.
[98] S. Arumugam, V. V. Popik, *J. Am. Chem. Soc.* **2012**, *134*, 8408 – 8411.
[99] K. Hiltebrandt, T. Pauloehrl, J. P. Blinco, K. Linkert, H. G. Börner, C. Barner-Kowollik, *Angew. Chem. Int. Ed.* **2015**, *54*, 2838 – 2843; *Angew. Chem.* **2015**, *127*, 2880 – 2885.
[100] N. Zydziak, F. Feist, B. Huber, J. O. Mueller, C. Barner-Kowollik, *Chem. Commun.* **2015**, *51*, 1799 – 1802.

Received: May 30, 2015
Published online: September 1, 2015

